Appl Phys B (2011) 102: 215–224
DOI 10.1007/s00340-010-4156-x

Applied Physics B
Lasers and Optics

Analytic vectorial structure of circular flattened Gaussian beams

G. Zhou · X. Chu

Received: 22 March 2010 / Revised version: 12 June 2010 / Published online: 11 August 2010

Abstract By means of the method of vector angular spectrum representation and the mathematical techniques, the analytically vectorial structure of the circular flattened Gaussian beam (CFGB) is derived without any approximation, which can be applicable to an arbitrary observation plane. In the far-field, the analytical formulae of the TE and the TM terms are further simplified using the method of stationary phase. The analytical expressions of the energy flux for the TE term, the TM term, and the CFGB are also presented. The energy flux distributions of the TE term, the TM term, and the CFGB are demonstrated in different reference planes, and the evolvement of the patterns of the TE term, the TM term, and the CFGB upon propagation are graphically illustrated.

1 Introduction

The flattened beams, namely the optical beams with a nearly uniform intensity distribution, are required in some certain applications [1] and have attracted a lot of attention. The propagation properties of flattened beams including the propagation factor and the kurtosis parameter have been investigated in free space [2, 3]. The focal shift of focused flattened beams has been examined [4]. The propagation characteristics of flattened beams have been demonstrated in the fractional Fourier transform plane [5, 6]. The analytical expressions for flattened beams through a misaligned or an apertured or an unapertured *ABCD* optical system have been derived, the corresponding propagation properties have been extensively discussed [7–13]. The propagation of flattened beams in the turbulent atmosphere, which includes the average intensity distribution and the scintillation index, has been investigated in detail [14–19]. The flattened beams can be experimentally generated by double-pass copper vapor laser masteroscillator power-amplifier systems [20] and another efficient optical system [21]. To describe the flattened beams, many different theoretical models have been proposed [22–27], one of which, namely a circular flattened Gaussian beam (CFGB), is a suitable one [28, 29]. The advantage of the CFGB is that the intensity distribution is varied from the flattened center to zero in a continuous and nonoscillatory way. The propagation of a CFGB with and without a circular aperture through an optical system is investigated in the turbulent atmosphere [30, 31]. To further examine the propagation properties of a CFGB, the vectorial structure of a CFGB is investigated in this paper. According to the value of the axial propagation distance, the beam propagation region is divided into the three regions [32]: the source region (the axial propagation distance smaller than or of the order of the wavelength), the near-field (the axial propagation distance larger than a few wavelengths), and the far-field (the axial propagation distance approaching infinity). If the vectorial structure of a CFGB presented here is applicable arbitrarily to any of the three propagation regions, one can examine the variational rule of the CFGB upon propagation. To achieve the above goal, here the description of a CFGB is based on the method of vector angular spectrum representation. By means of some mathematical techniques, the vectorial structure of a CFGB is derived without any approximation. By using the formulae derived, the energy flux distributions of the CFGB and its structural composition are numerically investigated.

G. Zhou (✉) · X. Chu
School of Sciences, Zhejiang A & F University, Lin'an 311300, Zhejiang Province, China
e-mail: zhouguoquan178@sohu.com

2 Analytically vectorial structure of CFGBs

In the Cartesian coordinate system, a CFGB propagates toward half free space $z \geq 0$. The z-axis is taken to be the propagation axis. In the theoretical researches and the practical applications, the linearly polarized state is the familiar and simple case. Therefore, the initial electric field of a CFGB in the source plane $z = 0$ is assumed to be polarized in the x-direction and takes the form of [28, 29]

$$\begin{pmatrix} E_x(\rho_0, 0) \\ E_y(\rho_0, 0) \end{pmatrix} = \begin{pmatrix} \sum_{m=1}^{N} b_m \exp(-\frac{m\rho_0^2}{w_0^2}) \\ 0 \end{pmatrix} \tag{1}$$

with the weight coefficient b_m given by

$$b_m = \frac{(-1)^{m-1}}{N} \binom{N}{m}, \tag{2}$$

where the integer $N \geq 2$ and $\rho_0 = (x_0^2 + y_0^2)^{1/2}$. $w_0/\sqrt{m}$ is the Gaussian waist. The flatness of the beam profile of a CFGB in the source plane is mainly determined by the parameter N. Increasing the parameter N effectively flattens the beam more. According to the vector angular spectrum representation of an electromagnetic beam, the propagating electric field of the CFGB can be written as

$$\boldsymbol{E}(\rho, z) = \int_{-\infty}^{\infty}\int_{-\infty}^{\infty} \boldsymbol{A}(p, q) \times \exp\big[ik(px + qy + \gamma z)\big]\, dp\, dq, \tag{3}$$

where

$$\boldsymbol{A}(p, q) = A_x(p, q)\left(\boldsymbol{e}_x - \frac{p}{\gamma}\boldsymbol{e}_z\right), \tag{4}$$

and

$$\begin{aligned} A_x(p, q) &= \frac{1}{\lambda^2}\int_{-\infty}^{\infty}\int_{-\infty}^{\infty} E_x(\rho_0, 0) \times \exp\big[-ik(px_0 + qy_0)\big]\, dx_0\, dy_0 \\ &= \frac{1}{4\pi f^2}\sum_{m=1}^{N}\frac{b_m}{m}\exp\left(-\frac{\beta^2}{4mf^2}\right). \end{aligned} \tag{5}$$

$\boldsymbol{A}(p, q)$ is the vector angular spectrum and $k = 2\pi/\lambda$ with λ the optical wavelength. $\boldsymbol{e}_x$ and $\boldsymbol{e}_z$ are the two unit vectors in the x- and z-directions, respectively. $\rho = (x^2 + y^2)^{1/2}$, $\beta = (p^2 + q^2)^{1/2}$, $\gamma = (1 - \beta^2)^{1/2}$, and $f = 1/kw_0$. The values of $\beta < 1$ correspond to the homogeneous plane waves propagating at angles $\sin^{-1}\beta$ with respect to the z-axis, whereas values of $\beta > 1$ correspond to the evanescent waves. The time dependent factor $\exp(-i\omega t)$ is omitted in (3), and ω is the angular frequency.

In the frequency domain, we can define two unit vectors $\boldsymbol{e}_1$ and $\boldsymbol{e}_2$ as [33–36]:

$$\boldsymbol{e}_1 = \frac{q}{\beta}\boldsymbol{e}_x - \frac{p}{\beta}\boldsymbol{e}_y, \qquad \boldsymbol{e}_2 = \frac{p\gamma}{\beta}\boldsymbol{e}_x + \frac{q\gamma}{\beta}\boldsymbol{e}_y - \beta\boldsymbol{e}_z, \tag{6}$$

where $\boldsymbol{e}_y$ is the unit vector in the y-direction. The three unit vectors $\boldsymbol{s}, \boldsymbol{e}_1$, and $\boldsymbol{e}_2$ form a mutually perpendicular right-handed system:

$$\boldsymbol{s} \times \boldsymbol{e}_1 = \boldsymbol{e}_2, \qquad \boldsymbol{e}_1 \times \boldsymbol{e}_2 = \boldsymbol{s}, \qquad \boldsymbol{e}_2 \times \boldsymbol{s} = \boldsymbol{e}_1, \tag{7}$$

where $\boldsymbol{s} = p\boldsymbol{e}_x + q\boldsymbol{e}_y + \gamma\boldsymbol{e}_z$. In this frequency domain, the vector angular spectrum $\boldsymbol{A}(p, q)$ can be decomposed into two terms [33–36]:

$$\boldsymbol{A}(p, q) = \big[\boldsymbol{A}(p, q) \cdot \boldsymbol{e}_1\big]\boldsymbol{e}_1 + \big[\boldsymbol{A}(p, q) \cdot \boldsymbol{e}_2\big]\boldsymbol{e}_2, \tag{8}$$

where the dot denotes the scalar product. Accordingly, the propagating electric field of a CFGB can be expressed as a sum of the TE and TM terms:

$$\boldsymbol{E}(\rho, z) = \boldsymbol{E}_{\mathrm{TE}}(\rho, z) + \boldsymbol{E}_{\mathrm{TM}}(\rho, z), \tag{9}$$

with $\boldsymbol{E}_{\mathrm{TE}}(\rho, z)$ and $\boldsymbol{E}_{\mathrm{TM}}(\rho, z)$ given by

$$\boldsymbol{E}_{\mathrm{TE}}(\rho, z) = \int_{-\infty}^{\infty}\int_{-\infty}^{\infty}\big[\boldsymbol{A}(p, q) \cdot \boldsymbol{e}_1\big]\boldsymbol{e}_1 \times \exp\big[ik(px + qy + \gamma z)\big]\, dp\, dq, \tag{10}$$

$$\boldsymbol{E}_{\mathrm{TM}}(\rho, z) = \int_{-\infty}^{\infty}\int_{-\infty}^{\infty}\big[\boldsymbol{A}(p, q) \cdot \boldsymbol{e}_2\big]\boldsymbol{e}_2 \times \exp\big[ik(px + qy + \gamma z)\big]\, dp\, dq. \tag{11}$$

The corresponding magnetic field of a CFGB can also be expressed as a sum of the TE and TM terms:

$$\boldsymbol{H}(\rho, z) = \boldsymbol{H}_{\mathrm{TE}}(\rho, z) + \boldsymbol{H}_{\mathrm{TM}}(\rho, z), \tag{12}$$

with $\boldsymbol{H}_{\mathrm{TE}}(\rho, z)$ and $\boldsymbol{H}_{\mathrm{TM}}(\rho, z)$ given by

$$\boldsymbol{H}_{\mathrm{TE}}(\rho, z) = \eta\int_{-\infty}^{\infty}\int_{-\infty}^{\infty}\big[\boldsymbol{A}(p, q) \cdot \boldsymbol{e}_1\big]\boldsymbol{e}_2 \times \exp\big[ik(px + qy + \gamma z)\big]\, dp\, dq, \tag{13}$$

$$\boldsymbol{H}_{\mathrm{TM}}(\rho, z) = -\eta\int_{-\infty}^{\infty}\int_{-\infty}^{\infty}\big[\boldsymbol{A}(p, q) \cdot \boldsymbol{e}_2\big]\boldsymbol{e}_1 \times \exp\big[ik(px + qy + \gamma z)\big]\, dp\, dq, \tag{14}$$

where $\eta = (\varepsilon_0/\mu_0)^{1/2}$. ε_0 and μ_0 are the electric permittivity and the magnetic permeability of vacuum, respectively. Here, the TE and TM terms denote that the longitudinal component of the electric and the magnetic fields is equal to zero, respectively. Inserting (4)–(6) into (10), the TE term

of the propagating electric field for a CFGB yields

$$\boldsymbol{E}_{\mathrm{TE}}(\rho,z)=\frac{1}{8\pi f^2}\sum_{m=1}^{N}\frac{b_m}{m}\int_0^{\infty}\int_0^{2\pi}\exp\left(-\frac{\beta^2}{4mf^2}\right)\times\left(2\sin^2\varphi\boldsymbol{e}_x-\sin 2\varphi\boldsymbol{e}_y\right)\exp(ik\gamma z)\times\exp\left[ik\rho\beta\cos(\varphi-\theta)\right]\beta\,d\beta\,d\varphi, \tag{15}$$

where $\theta=\tan^{-1}(y/x)$ and $\varphi=\tan^{-1}(q/p)$. By evaluating the integral over φ, (15) turns out to

$$\boldsymbol{E}_{\mathrm{TE}}(\rho,z)=\frac{1}{4f^2}\sum_{m=1}^{N}\frac{b_m}{m}\left\{\left[T_0(\rho,z)+\cos 2\theta T_2(\rho,z)\right]\boldsymbol{e}_x+\sin 2\theta T_2(\rho,z)\boldsymbol{e}_y\right\}, \tag{16}$$

with $T_{2n}(\rho,z)$ given by

$$T_{2n}(\rho,z)=\int_0^{\infty}\exp\left(-\frac{\beta^2}{4mf^2}\right)\exp(ik\gamma z)\times J_{2n}(k\rho\beta)\beta\,d\beta, \tag{17}$$

where J_{2n} is the $2n$-th order Bessel function of the first kind, and n is an arbitrary integer. Similarly, the TM term of the propagating electric field for a CFGB reads as

$$\boldsymbol{E}_{\mathrm{TM}}(\rho,z)=\frac{1}{4f^2}\sum_{m=1}^{N}\frac{b_m}{m}\left\{\left[T_0(\rho,z)-\cos 2\theta T_2(\rho,z)\right]\boldsymbol{e}_x-\sin 2\theta T_2(\rho,z)\boldsymbol{e}_y-i2\cos\theta U(\rho,z)\boldsymbol{e}_z\right\}, \tag{18}$$

with $U(\rho,z)$ given by

$$U(\rho,z)=\int_0^{\infty}\exp\left(-\frac{\beta^2}{4mf^2}\right)\exp(ik\gamma z)\times J_1(k\rho\beta)\beta^2\gamma^{-1}\,d\beta. \tag{19}$$

The TE and TM terms of the propagating magnetic field for a CFGB are found to be

$$\boldsymbol{H}_{\mathrm{TE}}(\rho,z)=\frac{\eta}{4f^2}\sum_{m=1}^{N}\frac{b_m}{m}\left\{\sin 2\theta G_2(\rho,z)\boldsymbol{e}_x+\left[G_0(\rho,z)+\cos 2\theta G_2(\rho,z)\right]\boldsymbol{e}_y-T_0(\rho,z)\boldsymbol{e}_z\right\}, \tag{20}$$

$$\boldsymbol{H}_{\mathrm{TM}}(\rho,z)=-\frac{\eta}{4f^2}\sum_{m=1}^{N}\frac{b_m}{m}\left\{\sin 2\theta K_2(\rho,z)\boldsymbol{e}_x-\left[K_0(\rho,z)-\cos 2\theta K_2(\rho,z)\right]\boldsymbol{e}_y\right\}, \tag{21}$$

with $G_{2n}(\rho,z)$ and $K_{2n}(\rho,z)$ given by

$$G_{2n}(\rho,z)=\int_0^{\infty}\exp\left(-\frac{\beta^2}{4mf^2}\right)\exp(ik\gamma z)\times J_{2n}(k\rho\beta)\beta\gamma\,d\beta, \tag{22}$$

$$K_{2n}(\rho,z)=\int_0^{\infty}\exp\left(-\frac{\beta^2}{4mf^2}\right)\exp(ik\gamma z)\times J_{2n}(k\rho\beta)\beta\gamma^{-1}d\beta. \tag{23}$$

In the source region, z is smaller than or of the order of the wavelength. Accordingly, the homogeneous and the evanescent plane waves must be both taken into account for the contribution to the electromagnetic field. By transforming the integral variable from β to γ, (17), (19), (22), and (23) can be rewritten as

$$T_{2n}(\rho,z)=\delta_m\left[\int_0^1\exp\left(\frac{\gamma^2}{4mf^2}\right)\exp(ik\gamma z)\times J_{2n}\left(k\rho\sqrt{1-\gamma^2}\right)\gamma\,d\gamma-\int_0^{+i\infty}\exp\left(\frac{\gamma^2}{4mf^2}\right)\times\exp(ik\gamma z)J_{2n}\left(k\rho\sqrt{1-\gamma^2}\right)\gamma\,d\gamma\right], \tag{24}$$

$$U(\rho,z)=\delta_m\left[\int_0^1\exp\left(\frac{\gamma^2}{4mf^2}\right)\exp(ik\gamma z)J_1\left(k\rho\sqrt{1-\gamma^2}\right)\times\sqrt{1-\gamma^2}\,d\gamma-\int_0^{+i\infty}\exp\left(\frac{\gamma^2}{4mf^2}\right)\exp(ik\gamma z)\times J_1\left(k\rho\sqrt{1-\gamma^2}\right)\sqrt{1-\gamma^2}\,d\gamma\right], \tag{25}$$

$$G_{2n}(\rho,z)=\delta_m\left[\int_0^1\exp\left(\frac{\gamma^2}{4mf^2}\right)\exp(ik\gamma z)\times J_{2n}\left(k\rho\sqrt{1-\gamma^2}\right)\gamma^2\,d\gamma-\int_0^{+i\infty}\exp\left(\frac{\gamma^2}{4mf^2}\right)\exp(ik\gamma z)\times J_{2n}\left(k\rho\sqrt{1-\gamma^2}\right)\gamma^2\,d\gamma\right], \tag{26}$$

$$K_{2n}(\rho,z)=\delta_m\left[\int_0^1\exp\left(\frac{\gamma^2}{4mf^2}\right)\exp(ik\gamma z)\times J_{2n}\left(k\rho\sqrt{1-\gamma^2}\right)d\gamma-\int_0^{+i\infty}\exp\left(\frac{\gamma^2}{4mf^2}\right)\times\exp(ik\gamma z)J_{2n}\left(k\rho\sqrt{1-\gamma^2}\right)d\gamma\right], \tag{27}$$

where $\delta_m=\exp(-1/4mf^2)$. The above equations are difficult for directly computing the integral. However, the fol-

lowing Taylor expansions are valid [37]:

$$J_{2n}\left(k\rho\sqrt{1-\gamma^2}\right) = \left(\frac{k\rho}{2}\right)^{2n}\sum_{l=0}^{\infty}\sum_{s=0}^{l+n}\frac{(-1)^s c_l (l+n)!\gamma^{2s}}{s!(l+2n)!(l-s+n)!}, \tag{28}$$

$$J_1\left(k\rho\sqrt{1-\gamma^2}\right)\sqrt{1-\gamma^2} = \frac{k\rho}{2}\sum_{l=0}^{\infty}\sum_{s=0}^{l+1}\frac{(-1)^s c_l \gamma^{2s}}{s!(l+1-s)!}, \tag{29}$$

where $c_l = (-1)^l (k\rho/2)^{2l}/l!$. Therefore, (24) yields

$$T_{2n}(\rho,z) = \delta_m\left(\frac{k\rho}{2}\right)^{2n} \times \sum_{l=0}^{\infty}\sum_{s=0}^{l+n}\frac{(-1)^s c_l (l+n)!(I^{\text{pro}}_{2s+1} - I^{\text{eve}}_{2s+1})}{s!(l+2n)!(l-s+n)!}, \tag{30}$$

with I_j^{pro} and I_j^{eve} given by

$$I_j^{\text{pro}} = \int_0^1 \exp\left(\frac{\gamma^2}{4mf^2}\right)\exp(ik\gamma z)\gamma^j d\gamma = 2mf^2\left[\exp\left(\frac{1}{4mf^2}+ikz\right) - ikzI_{j-1}^{\text{pro}} - (j-1)I_{j-2}^{\text{pro}}\right], \tag{31}$$

$$I_0^{\text{pro}} = if\sqrt{m\pi}\left[F\left(i\sqrt{m}kfz\right) - \exp\left(\frac{1}{4mf^2}+ikz\right) \times F\left(i\sqrt{m}kfz + \frac{1}{2\sqrt{m}f}\right)\right], \tag{32}$$

$$I_1^{\text{pro}} = 2mf^2\left[\exp\left(\frac{1}{4mf^2}+ikz\right) - 1 - ikzI_0^{\text{pro}}\right], \tag{33}$$

$$I_j^{\text{eve}} = \int_0^{+i\infty}\exp\left(\frac{\gamma^2}{4mf^2}\right)\exp(ik\gamma z)\gamma^j d\gamma = \left(i\sqrt{2m}f\right)^{j+1} j! D_{j+1}\left(\sqrt{2}mkfz\right), \tag{34}$$

where j is an arbitrary integer. $F(\cdot)$ is the Faddeev function and is calculated by the procedure suggested by [38]. $D_{j+1}(\cdot)$ is related to the parabolic cylinder function. The recurrence relation of $D_{j+1}(x)$ is given by [37]

$$D_1(x) = \sqrt{\frac{\pi}{2}}F\left(i\frac{x}{\sqrt{2}}\right), \tag{35}$$

$$D_2(x) = 1 - xD_1(x), \tag{36}$$

$$D_{j+1}(x) = \frac{1}{j}\left[D_{j-1}(x) - xD_j(x)\right]. \tag{37}$$

Similarly, (25)–(27) turn out to be

$$U(\rho,z) = \frac{k\delta_m\rho}{2}\sum_{l=0}^{\infty}\sum_{s=0}^{l+1}\frac{(-1)^s c_l (I^{\text{pro}}_{2s} - I^{\text{eve}}_{2s})}{s!(l+1-s)!}, \tag{38}$$

$$G_{2n}(\rho,z) = \delta_m\left(\frac{k\rho}{2}\right)^{2n} \times \sum_{l=0}^{\infty}\sum_{s=0}^{l+n}\frac{(-1)^s c_l (l+n)!(I^{\text{pro}}_{2s+2} - I^{\text{eve}}_{2s+2})}{s!(l+2n)!(l-s+n)!}, \tag{39}$$

$$K_{2n}(\rho,z) = \delta_m\left(\frac{k\rho}{2}\right)^{2n} \times \sum_{l=0}^{\infty}\sum_{s=0}^{l+n}\frac{(-1)^s c_l (l+n)!(I^{\text{pro}}_{2s} - I^{\text{eve}}_{2s})}{s!(l+2n)!(l-s+n)!}. \tag{40}$$

Therefore, the analytical expression of the TE term of the propagating electric field for a CFGB reads as

$$\boldsymbol{E}_{\text{TE}}(\rho,z) = \boldsymbol{E}^{\text{pro}}_{\text{TE}}(\rho,z) + \boldsymbol{E}^{\text{eve}}_{\text{TE}}(\rho,z), \tag{41}$$

with $\boldsymbol{E}^{\text{pro}}_{\text{TE}}(\rho,z)$ and $\boldsymbol{E}^{\text{eve}}_{\text{TE}}(\rho,z)$given by

$$\boldsymbol{E}^{\text{pro}}_{\text{TE}}(\rho,z) = \sum_{m=1}^{N}\frac{a_m b_m}{m}\left(\sum_{l=0}^{\infty}\sum_{s=0}^{l}\frac{(-1)^s c_l I^{\text{pro}}_{2s+1}}{s!(l-s)!}\boldsymbol{e}_x + \frac{k^2\rho^2}{4}(\cos 2\theta\boldsymbol{e}_x + \sin 2\theta\boldsymbol{e}_y) \times \sum_{l=0}^{\infty}\sum_{s=0}^{l+1}\frac{(-1)^s c_l I^{\text{pro}}_{2s+1}}{(l+2)s!(l+1-s)!}\right), \tag{42}$$

$$\boldsymbol{E}^{\text{eve}}_{\text{TE}}(\rho,z) = -\sum_{m=1}^{N}\frac{a_m b_m}{m}\left(\sum_{l=0}^{\infty}\sum_{s=0}^{l}\frac{(-1)^s c_l I^{\text{eve}}_{2s+1}}{s!(l-s)!}\boldsymbol{e}_x + \frac{k^2\rho^2}{4}(\cos 2\theta\boldsymbol{e}_x + \sin 2\theta\boldsymbol{e}_y) \times \sum_{l=0}^{\infty}\sum_{s=0}^{l+1}\frac{(-1)^s c_l I^{\text{eve}}_{2s+1}}{(l+2)s!(l+1-s)!}\right), \tag{43}$$

where $a_m = \delta_m/4f^2$. Similarly, the analytical expression of the TM term of the propagating electric field for a CFGB yields

$$\boldsymbol{E}_{\text{TM}}(\rho,z) = \boldsymbol{E}^{\text{pro}}_{\text{TM}}(\rho,z) + \boldsymbol{E}^{\text{eve}}_{\text{TM}}(\rho,z), \tag{44}$$

with $\boldsymbol{E}^{\text{pro}}_{\text{TM}}(\rho,z)$ and $\boldsymbol{E}^{\text{eve}}_{\text{TM}}(\rho,z)$ given by

$$\boldsymbol{E}^{\text{pro}}_{\text{TM}}(\rho,z) = \sum_{m=1}^{N}\frac{a_m b_m}{m}\left(\sum_{l=0}^{\infty}\sum_{s=0}^{l}\frac{(-1)^s c_l I^{\text{pro}}_{2s+1}}{s!(l-s)!}\boldsymbol{e}_x - \frac{k^2\rho^2}{4}(\cos 2\theta\boldsymbol{e}_x + \sin 2\theta\boldsymbol{e}_y)\right.$$

$$\times \sum_{l=0}^{\infty}\sum_{s=0}^{l+1}\frac{(-1)^s c_l I_{2s+1}^{\mathrm{pro}}}{(l+2)s!(l+1-s)!} - i\cos\theta k\rho \sum_{l=0}^{\infty}\sum_{s=0}^{l+1}\frac{(-1)^s c_l I_{2s}^{\mathrm{pro}}}{s!(l+1-s)!}\boldsymbol{e}_z\Bigg), \quad (45)$$

$$\boldsymbol{E}_{\mathrm{TM}}^{\mathrm{eve}}(\rho,z) = -\sum_{m=1}^{N}\frac{a_m b_m}{m}\Bigg(\sum_{l=0}^{\infty}\sum_{s=0}^{l}\frac{(-1)^s c_l I_{2s+1}^{\mathrm{eve}}}{s!(l-s)!}\boldsymbol{e}_x - \frac{k^2\rho^2}{4}(\cos 2\theta\boldsymbol{e}_x + \sin 2\theta\boldsymbol{e}_y) \times \sum_{l=0}^{\infty}\sum_{s=0}^{l+1}\frac{(-1)^s c_l I_{2s+1}^{\mathrm{eve}}}{(l+2)s!(l+1-s)!} - i\cos\theta k\rho \sum_{l=0}^{\infty}\sum_{s=0}^{l+1}\frac{(-1)^s c_l I_{2s}^{\mathrm{eve}}}{s!(l+1-s)!}\boldsymbol{e}_z\Bigg). \quad (46)$$

The analytical expressions of the TE and the TM terms of the propagating magnetic field for a CFGB are found to be

$$\boldsymbol{H}_{\mathrm{TE}}(\rho,z) = \boldsymbol{H}_{\mathrm{TE}}^{\mathrm{pro}}(\rho,z) + \boldsymbol{H}_{\mathrm{TE}}^{\mathrm{eve}}(\rho,z), \quad (47)$$

$$\boldsymbol{H}_{\mathrm{TM}}(\rho,z) = \boldsymbol{H}_{\mathrm{TM}}^{\mathrm{pro}}(\rho,z) + \boldsymbol{H}_{\mathrm{TM}}^{\mathrm{eve}}(\rho,z), \quad (48)$$

with $\boldsymbol{H}_{\mathrm{TE}}^{\mathrm{pro}}(\rho,z)$, $\boldsymbol{H}_{\mathrm{TE}}^{\mathrm{eve}}(\rho,z)$, $\boldsymbol{H}_{\mathrm{TM}}^{\mathrm{pro}}(\rho,z)$, and $\boldsymbol{H}_{\mathrm{TM}}^{\mathrm{eve}}(\rho,z)$ given by

$$\boldsymbol{H}_{\mathrm{TE}}^{\mathrm{pro}}(\rho,z) = \eta\sum_{m=1}^{N}\frac{a_m b_m}{m}\Bigg(\frac{k^2\rho^2}{4}(\sin 2\theta\boldsymbol{e}_x + \cos 2\theta\boldsymbol{e}_y) \times \sum_{l=0}^{\infty}\sum_{s=0}^{l+1}\frac{(-1)^s c_l I_{2s+2}^{\mathrm{pro}}}{(l+2)s!(l+1-s)!} + \sum_{l=0}^{\infty}\sum_{s=0}^{l}\frac{(-1)^s c_l I_{2s+2}^{\mathrm{pro}}}{s!(l-s)!}\boldsymbol{e}_y - \sum_{l=0}^{\infty}\sum_{s=0}^{l}\frac{(-1)^s c_l I_{2s+1}^{\mathrm{pro}}}{s!(l-s)!}\boldsymbol{e}_z\Bigg), \quad (49)$$

$$\boldsymbol{H}_{\mathrm{TE}}^{\mathrm{eve}}(\rho,z) = -\eta\sum_{m=1}^{N}\frac{a_m b_m}{m}\Bigg(\frac{k^2\rho^2}{4}(\sin 2\theta\boldsymbol{e}_x + \cos 2\theta\boldsymbol{e}_y) \times \sum_{l=0}^{\infty}\sum_{s=0}^{l+1}\frac{(-1)^s c_l I_{2s+2}^{\mathrm{eve}}}{(l+2)s!(l+1-s)!} + \sum_{l=0}^{\infty}\sum_{s=0}^{l}\frac{(-1)^s c_l I_{2s+2}^{\mathrm{eve}}}{s!(l-s)!}\boldsymbol{e}_y - \sum_{l=0}^{\infty}\sum_{s=0}^{l}\frac{(-1)^s c_l I_{2s+1}^{\mathrm{eve}}}{s!(l-s)!}\boldsymbol{e}_z\Bigg), \quad (50)$$

$$\boldsymbol{H}_{\mathrm{TM}}^{\mathrm{pro}}(\rho,z) = -\eta\sum_{m=1}^{N}\frac{a_m b_m}{m}\Bigg(\frac{k^2\rho^2}{4}(\sin 2\theta\boldsymbol{e}_x + \cos 2\theta\boldsymbol{e}_y) \times \sum_{l=0}^{\infty}\sum_{s=0}^{l+1}\frac{(-1)^s c_l I_{2s}^{\mathrm{pro}}}{(l+2)s!(l+1-s)!} - \sum_{l=0}^{\infty}\sum_{s=0}^{l}\frac{(-1)^s c_l I_{2s}^{\mathrm{pro}}}{s!(l-s)!}\boldsymbol{e}_y\Bigg), \quad (51)$$

$$\boldsymbol{H}_{\mathrm{TM}}^{\mathrm{eve}}(\rho,z) = \eta\sum_{m=1}^{N}\frac{a_m b_m}{m}\Bigg(\frac{k^2\rho^2}{4}(\sin 2\theta\boldsymbol{e}_x + \cos 2\theta\boldsymbol{e}_y) \times \sum_{l=0}^{\infty}\sum_{s=0}^{l+1}\frac{(-1)^s c_l I_{2s}^{\mathrm{eve}}}{(l+2)s!(l+1-s)!} - \sum_{l=0}^{\infty}\sum_{s=0}^{l}\frac{(-1)^s c_l I_{2s}^{\mathrm{eve}}}{s!(l-s)!}\boldsymbol{e}_y\Bigg). \quad (52)$$

All above presented series are alternating and absolutely convergent. Moreover, the series associated with the propagating parts converge more quickly than those associated with the evanescent parts [39, 40]. Here, the analytical expressions of the TE and the TM terms are obtained without any approximation, which allows one to calculate them in an arbitrary observation plane.

In the far-field regime, the evanescent plane waves have completely disappeared, which means that the integral in (16) should be restrained within the range of $0 < \beta < 1$. According to the method of stationary phase [41], the analytical TE and TM terms in the far-field plane reduce to

$$\boldsymbol{E}_{\mathrm{TE}}(\rho,z) = -\frac{iz_r yz}{\rho^2 r^2}\exp(ikr)(y\boldsymbol{e}_x - x\boldsymbol{e}_y) \times \sum_{m=1}^{N}\frac{b_m}{m}\exp\left(-\frac{\rho^2}{4mf^2r^2}\right), \quad (53)$$

$$\boldsymbol{H}_{\mathrm{TE}}(\rho,z) = -\frac{i\eta z_r yz}{\rho^2 r^3}\exp(ikr)\left(xz\boldsymbol{e}_x + yz\boldsymbol{e}_y - \rho^2\boldsymbol{e}_z\right) \times \sum_{m=1}^{N}\frac{b_m}{m}\exp\left(-\frac{\rho^2}{4mf^2r^2}\right), \quad (54)$$

$$\boldsymbol{E}_{\mathrm{TM}}(\rho,z) = -\frac{iz_r x}{\rho^2 r^2}\exp(ikr)\left(xz\boldsymbol{e}_x + yz\boldsymbol{e}_y - \rho^2\boldsymbol{e}_z\right) \times \sum_{m=1}^{N}\frac{b_m}{m}\exp\left(-\frac{\rho^2}{4mf^2r^2}\right), \quad (55)$$

$$\boldsymbol{H}_{\mathrm{TM}}(\rho,z) = \frac{i\eta z_r x}{\rho^2 r}\exp(ikr)\left(y\boldsymbol{e}_x - x\boldsymbol{e}_y\right) \times \sum_{m=1}^{N}\frac{b_m}{m}\exp\left(-\frac{\rho^2}{4mf^2r^2}\right), \quad (56)$$

where $z_r = kw_0^2/2$, and $r = (\rho^2 + z^2)^{1/2}$. In the far-field plane, the TE and TM terms are orthogonal to each other.

3 Energy flux distribution of a CFGB

The energy flux distributions of the TE and TM terms for a CFGB are given by

$$\begin{aligned}\langle S_z\rangle_{\mathrm{TE}} &= \frac{1}{2}\mathrm{Re}\big[\boldsymbol{E}_{\mathrm{TE}}(\rho,z)\times\boldsymbol{H}^*_{\mathrm{TE}}(\rho,z)\big]_z \\ &= \eta\Bigg[\sum_{m=1}^{N}\frac{a_m b_m}{m}\Bigg(\sum_{l=0}^{\infty}\sum_{s=0}^{l}\frac{(-1)^s c_l(I^{\mathrm{pro}}_{2s+1}-I^{\mathrm{eve}}_{2s+1})}{s!(l-s)!} \\ &\quad+\frac{k^2\rho^2\cos 2\theta}{4}\sum_{l=0}^{\infty}\sum_{s=0}^{l+1}\frac{(-1)^s c_l(I^{\mathrm{pro}}_{2s+1}-I^{\mathrm{eve}}_{2s+1})}{(l+2)s!(l+1-s)!}\Bigg) \\ &\quad\times\sum_{m=1}^{N}\frac{a_m b_m}{m}\Bigg(\sum_{l=0}^{\infty}\sum_{s=0}^{l}\frac{(-1)^s c_l(I^{\mathrm{pro}}_{2s+2}-I^{\mathrm{eve}}_{2s+2})}{s!(l-s)!} \\ &\quad+\frac{k^2\rho^2\cos 2\theta}{4}\sum_{l=0}^{\infty}\sum_{s=0}^{l+1}\frac{(-1)^s c_l(I^{\mathrm{pro}}_{2s+2}-I^{\mathrm{eve}}_{2s+2})}{(l+2)s!(l+1-s)!}\Bigg) \\ &\quad-\frac{k^4\rho^4\sin^2 2\theta}{16}\sum_{m=1}^{N}\sum_{l=0}^{\infty}\sum_{s=0}^{l+1}\frac{a_m b_m}{m} \\ &\quad\times\frac{(-1)^s c_l(I^{\mathrm{pro}}_{2s+1}-I^{\mathrm{eve}}_{2s+1})}{(l+2)s!(l+1-s)!}\sum_{m=1}^{N}\sum_{l=0}^{\infty}\sum_{s=0}^{l+1}\frac{a_m b_m}{m} \\ &\quad\times\frac{(-1)^s c_l(I^{\mathrm{pro}}_{2s+2}-I^{\mathrm{eve}}_{2s+2})}{(l+2)s!(l+1-s)!}\Bigg], \end{aligned} \tag{57}$$

$$\begin{aligned}\langle S_z\rangle_{\mathrm{TM}} &= \eta\Bigg[\sum_{m=1}^{N}\frac{a_m b_m}{m}\Bigg(\sum_{l=0}^{\infty}\sum_{s=0}^{l}\frac{(-1)^s c_l(I^{\mathrm{pro}}_{2s+1}-I^{\mathrm{eve}}_{2s+1})}{s!(l-s)!} \\ &\quad-\frac{k^2\rho^2\cos 2\theta}{4}\sum_{l=0}^{\infty}\sum_{s=0}^{l+1}\frac{(-1)^s c_l(I^{\mathrm{pro}}_{2s+1}-I^{\mathrm{eve}}_{2s+1})}{(l+2)s!(l+1-s)!}\Bigg) \\ &\quad\times\sum_{m=1}^{N}\frac{a_m b_m}{m}\Bigg(\sum_{l=0}^{\infty}\sum_{s=0}^{l}\frac{(-1)^s c_l(I^{\mathrm{pro}}_{2s}-I^{\mathrm{eve}}_{2s})}{s!(l-s)!} \\ &\quad-\frac{k^2\rho^2\cos 2\theta}{4}\sum_{l=0}^{\infty}\sum_{s=0}^{l+1}\frac{(-1)^s c_l(I^{\mathrm{pro}}_{2s}-I^{\mathrm{eve}}_{2s})}{(l+2)s!(l+1-s)!}\Bigg) \\ &\quad-\frac{k^4\rho^4\sin^2 2\theta}{16} \\ &\quad\times\sum_{m=1}^{N}\sum_{l=0}^{\infty}\sum_{s=0}^{l+1}\frac{a_m b_m}{m}\frac{(-1)^s c_l(I^{\mathrm{pro}}_{2s+1}-I^{\mathrm{eve}}_{2s+1})}{(l+2)s!(l+1-s)!} \\ &\quad\times\sum_{m=1}^{N}\sum_{l=0}^{\infty}\sum_{s=0}^{l+1}\frac{a_m b_m}{m}\frac{(-1)^s c_l(I^{\mathrm{pro}}_{2s}-I^{\mathrm{eve}}_{2s})}{(l+2)s!(l+1-s)!}\Bigg], \end{aligned} \tag{58}$$

where the angle brackets indicate an average with respect to the time variable t. Re denotes taking the real part, and the asterisk means the complex conjugation. The energy flux distribution of a CFGB is found to be

$$\begin{aligned}\langle S_z\rangle &= 2\eta\sum_{m=1}^{N}\sum_{l=0}^{\infty}\sum_{s=0}^{l}\frac{a_m b_m}{m}\frac{(-1)^s c_l(I^{\mathrm{pro}}_{2s+1}-I^{\mathrm{eve}}_{2s+1})}{s!(l-s)!} \\ &\quad\times\Bigg[\sum_{m=1}^{N}\frac{a_m b_m}{m}\Bigg(\sum_{l=0}^{\infty}\sum_{s=0}^{l}\frac{(-1)^s c_l(I^{\mathrm{pro}}_{2s+2}-I^{\mathrm{eve}}_{2s+2})}{s!(l-s)!} \\ &\quad+\frac{k^2\rho^2\cos 2\theta}{4}\sum_{l=0}^{\infty}\sum_{s=0}^{l+1}\frac{(-1)^s c_l(I^{\mathrm{pro}}_{2s+2}-I^{\mathrm{eve}}_{2s+2})}{(l+2)s!(l+1-s)!}\Bigg) \\ &\quad+\sum_{m=1}^{N}\frac{a_m b_m}{m}\Bigg(\sum_{l=0}^{\infty}\sum_{s=0}^{l}\frac{(-1)^s c_l(I^{\mathrm{pro}}_{2s}-I^{\mathrm{eve}}_{2s})}{s!(l-s)!} \\ &\quad-\frac{k^2\rho^2\cos 2\theta}{4}\sum_{l=0}^{\infty}\sum_{s=0}^{l+1}\frac{(-1)^s c_l(I^{\mathrm{pro}}_{2s}-I^{\mathrm{eve}}_{2s})}{(l+2)s!(l+1-s)!}\Bigg)\Bigg]. \end{aligned} \tag{59}$$

In the source region and the near-field, the TE and TM terms are not orthogonal to each other. Accordingly, there is a crossed energy flux caused by the unorthogonality of the vectorial structure:

$$\langle S_z\rangle = \langle S_z\rangle_{\mathrm{TE}} + \langle S_z\rangle_{\mathrm{TM}} + \langle S_z\rangle_{\mathrm{Cross}}. \tag{60}$$

The energy flux distributions of the TE and TM terms in the far-field plane are simplified to

$$\langle S_z\rangle_{\mathrm{TE}} = \frac{\eta z_r^2 y^2 z^3}{2\rho^2 r^5}\left[\sum_{m=1}^{N}\frac{b_m}{m}\exp\left(-\frac{\rho^2}{4mf^2r^2}\right)\right]^2, \tag{61}$$

$$\langle S_z\rangle_{\mathrm{TM}} = \frac{\eta z_r^2 x^2 z}{2\rho^2 r^3}\left[\sum_{m=1}^{N}\frac{b_m}{m}\exp\left(-\frac{\rho^2}{4mf^2r^2}\right)\right]^2. \tag{62}$$

As the electromagnetic fields of the TE and TM terms are orthogonal to each other in the far-field plane, the energy flux distribution of a CFGB reduces to

$$\begin{aligned}\langle S_z\rangle &= \langle S_z\rangle_{\mathrm{TE}} + \langle S_z\rangle_{\mathrm{TM}} \\ &= \frac{\eta z_r^2 z}{2\rho^2 r^3}\left(x^2+\frac{z^2}{r^2}y^2\right)\left[\sum_{m=1}^{N}\frac{b_m}{m}\exp\left(-\frac{\rho^2}{4mf^2r^2}\right)\right]^2. \end{aligned} \tag{63}$$

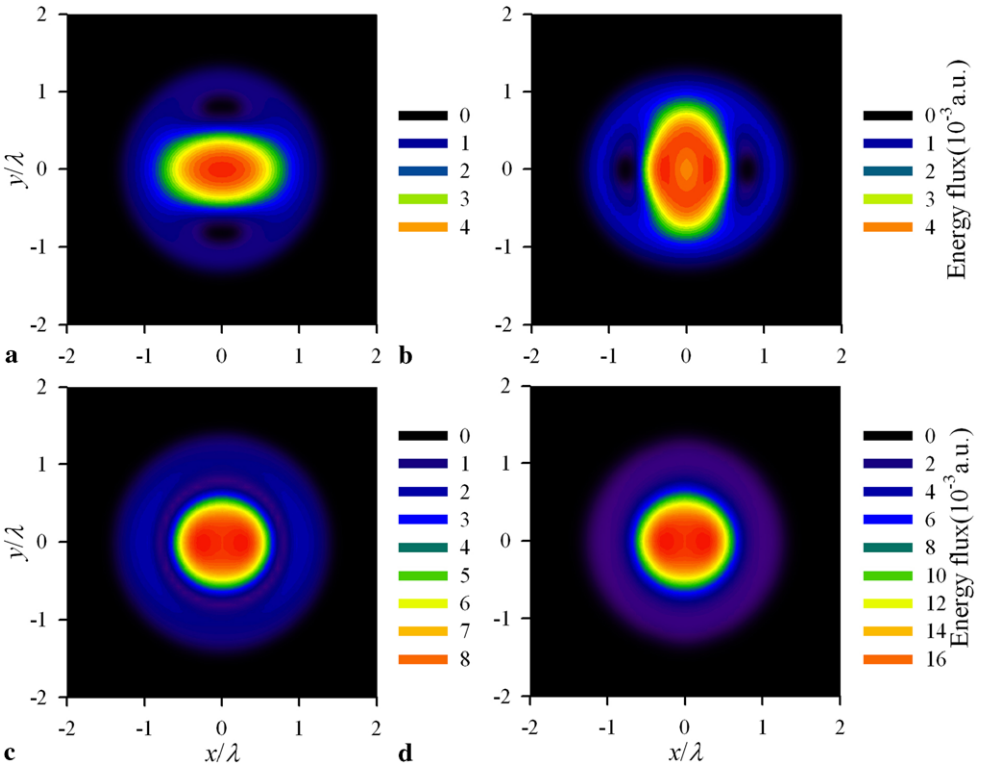

Fig. 1 Energy flux distribution of a CFGB in the reference plane $z = 0.05\lambda$. $N = 5$ and $w_0 = 0.5\lambda$: **a** $\langle S_z \rangle_{\mathrm{TE}}$, **b** $\langle S_z \rangle_{\mathrm{TM}}$, **c** $\langle S_z \rangle_{\mathrm{Cross}}$, **d** $\langle S_z \rangle$

4 Numerical calculations and analyses

The different parameters w_0 and N will result in the different distribution of the CFGB. Here the calculations are performed as examples. Therefore, the parameters w_0 and N are fixed to $N = 5$ and $w_0 = 0.5\lambda$. The description of optical propagation in the nonparaxial regime, dealing with values of w_0 such that $\lambda/w_0 > 1$, is becoming more and more important with the advent of new optical structures, like, e.g., microcavities and photonic bandgap crystals [42], possessing linear dimensions or spatial scales of variation comparable or even smaller than λ [43]. Therefore, here w_0 is set to 0.5λ. For simplicity, η is set to be unity in our calculations. The energy flux distributions of the TE term, the TM term, and the CFGB are plotted in the different reference planes and shown in Figs. 1–6. In Figs. 1–6, the reference plane is $z = 0.05\lambda, 0.10\lambda, 0.42\lambda, 5\lambda, 50\lambda$, and 1000λ, respectively. As $z = 0.05\lambda$ is very close to the source plane, the CFGB still has a circular flattened center, which is shown in Fig. 1. The magnitude of the energy flux distributions of the TE term is equal to that of the energy flux distributions of the TM term. The magnitude of the crossed energy flux is half of the magnitude of the whole beam. When $z = 0.10\lambda$ in Fig. 2, the pattern of the TE term is still the same as that in the plane of $z = 0.05\lambda$. However, the central region in the pattern of the TM term is no longer the maximum. Moreover, the magnitude of the energy flux distributions of the TM term is slightly larger than that of the energy flux distributions of the TE term. The center region in the crossed energy flux distribution is also not the maximum. As a result, the central region in the pattern of the whole beam is not the maximum. When $z = 0.42\lambda$ in Fig. 3, the pattern of the TM term can be approximately obtained by rotating the pattern of the TE term 90°. There is slight difference in the central spot between the patterns of the TE and the TM terms. As to the pattern of the whole beam, it is close to a Gaussian distribution. In Fig. 4, $z = 5\lambda$. In this case, the pattern of the TM term is just obtained by rotating the pattern of the TE term 90°. The pattern of the TE term is mainly composed of a central spot and three pairs of crescent side lobes. When $z = 50\lambda$ in Fig. 5, the crossed energy flux is confined to a small region. With increasing the axial propagation distance, the crossed energy flux decreases until disappears. In the far-field plane $z = 1000\lambda$, the pattern of the TE term in Fig. 6 is similar to a stuffed number of 8, and the pattern of the TM term in Fig. 6 is close to a stuffed symbol of ∞. Combining Fig. 6 with Figs. 3–5, we can find that the patterns of the TE term, the TM term, and the CFGB evolve towards the positive direction. As the CFGB is the supposition of N Gaussian beams with different Gaussian waists and different weight coefficients, the vectorial structure is complicated. Upon propagation, the patterns of the TE and TM terms are diverse.

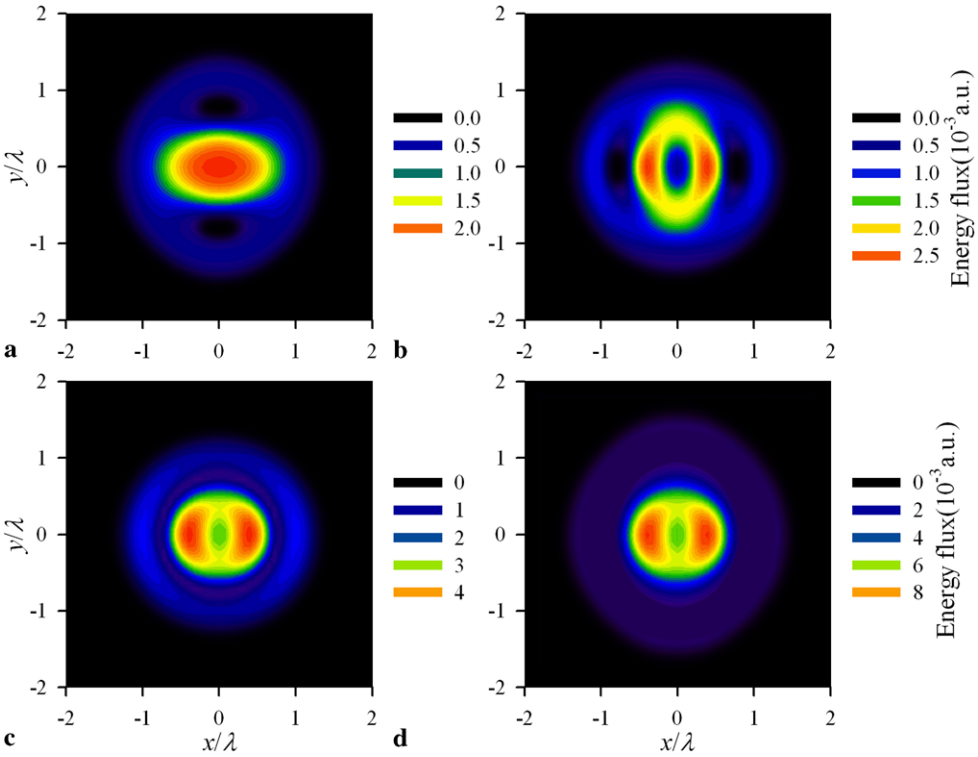

Fig. 2 Energy flux distribution of a CFGB in the reference plane $z = 0.10\lambda$. $N = 5$ and $w_0 = 0.5\lambda$: **a** $\langle S_z \rangle_{\mathrm{TE}}$, **b** $\langle S_z \rangle_{\mathrm{TM}}$, **c** $\langle S_z \rangle_{\mathrm{Cross}}$, **d** $\langle S_z \rangle$

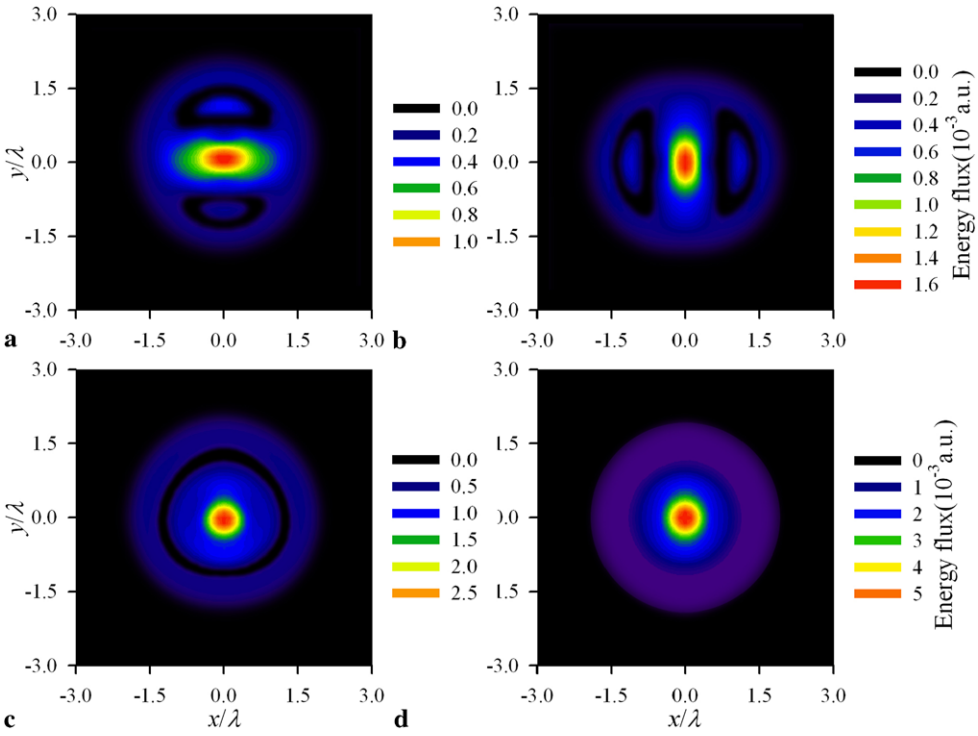

Fig. 3 Energy flux distribution of a CFGB in the reference plane $z = 0.42\lambda$. $N = 5$ and $w_0 = 0.5\lambda$: **a** $\langle S_z \rangle_{\mathrm{TE}}$, **b** $\langle S_z \rangle_{\mathrm{TM}}$, **c** $\langle S_z \rangle_{\mathrm{Cross}}$, **d** $\langle S_z \rangle$

5 Conclusions

By means of the method of vector angular spectrum representation and the mathematical techniques, the analytical vectorial structure of a CFGBB is derived without any approximation. Also, the accurate analytical expressions of the energy flux for the TE term, the TM term, and the CFGB are presented. In the far-field regime, the formulae are simplified by using the method of stationary phase. The vectorial structure of a CFGB presented here is applicable to an arbi-

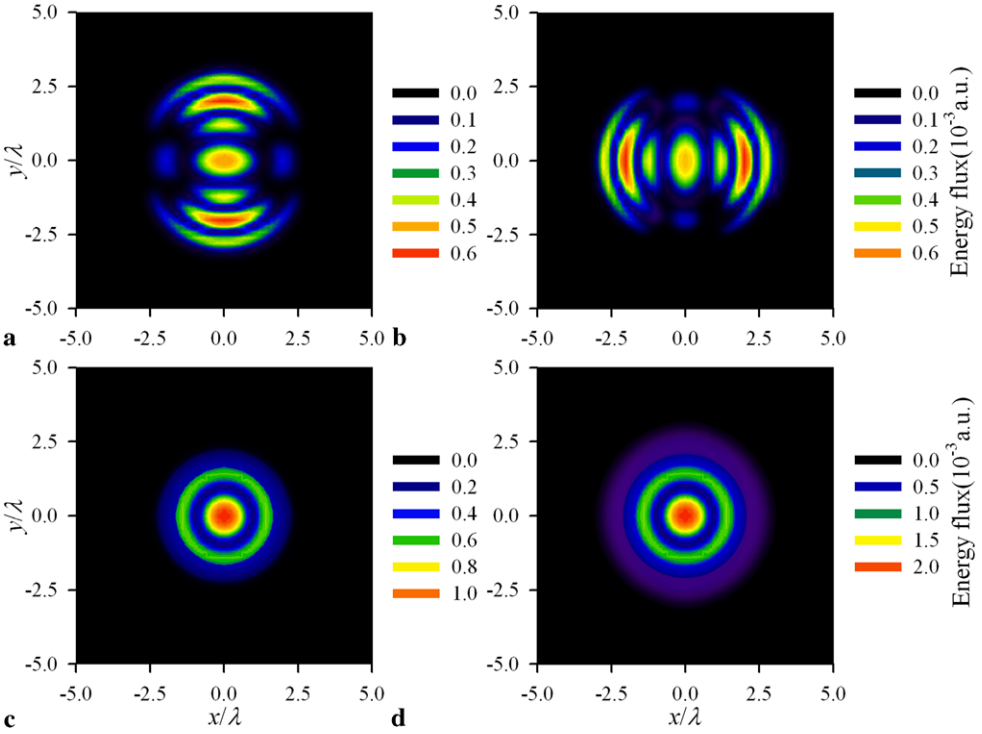

Fig. 4 Energy flux distribution of a CFGB in the reference plane $z = 5\lambda$. $N = 5$ and $w_0 = 0.5\lambda$: **a** $\langle S_z \rangle_{\mathrm{TE}}$, **b** $\langle S_z \rangle_{\mathrm{TM}}$, **c** $\langle S_z \rangle_{\mathrm{Cross}}$, **d** $\langle S_z \rangle$

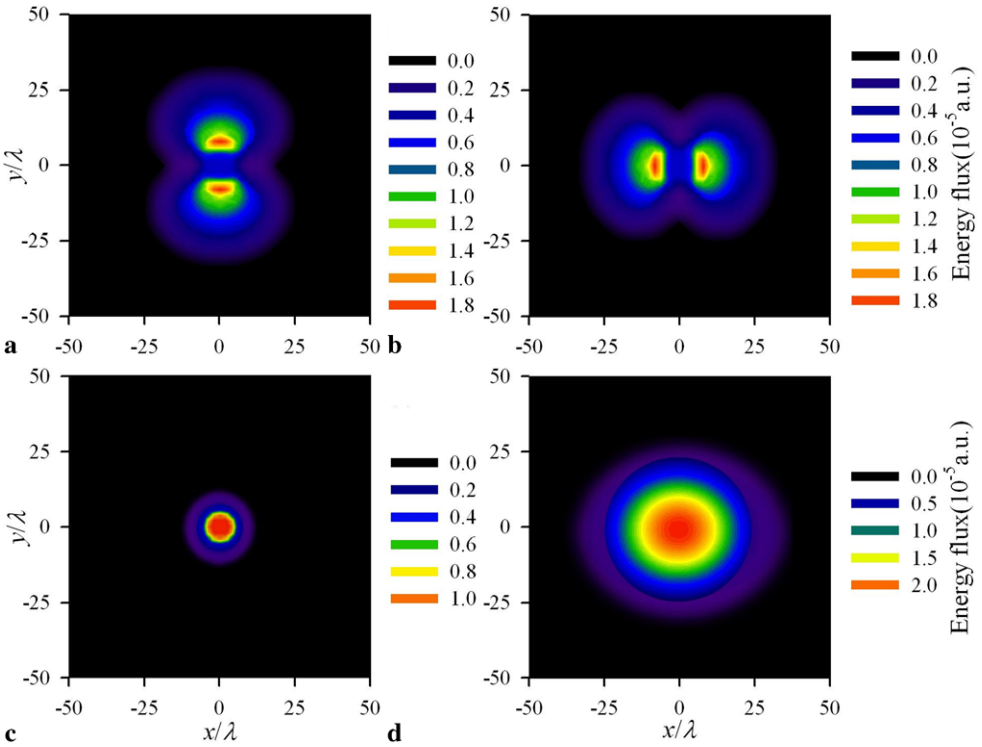

Fig. 5 Energy flux distribution of a CFGB in the reference plane $z = 50\lambda$. $N = 5$ and $w_0 = 0.5\lambda$: **a** $\langle S_z \rangle_{\mathrm{TE}}$, **b** $\langle S_z \rangle_{\mathrm{TM}}$, **c** $\langle S_z \rangle_{\mathrm{Cross}}$, **d** $\langle S_z \rangle$

trary propagation region. The energy flux distributions of the TE term, the TM term, and the CFGB are numerically depicted in the source region, the near-field, and the far-field, and the evolvement of the patterns of the TE term, the TM term, and the CFGB upon propagation are well illustrated. This research further reveals the propagation properties of a CFGB and is beneficial to the applications with a CFGB.

Acknowledgements This work was supported by Scientific Research Fund of Zhejiang Provincial Education Department. The authors are indebted to the reviewers for valuable comments.

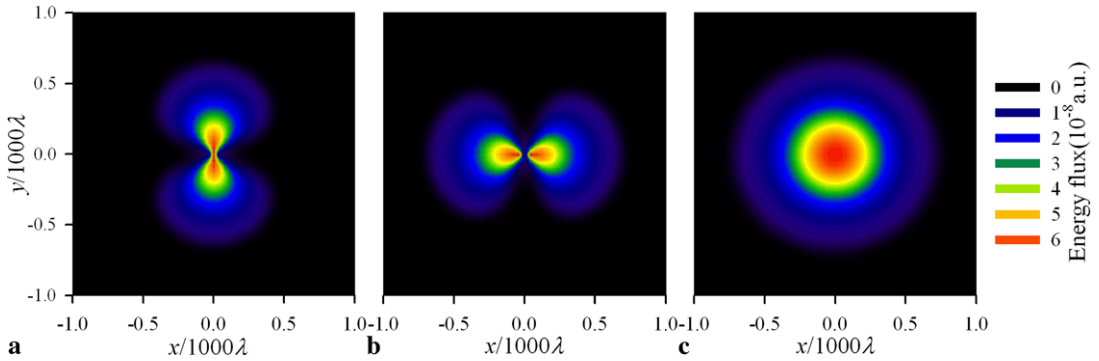

Fig. 6 Energy flux distribution of a CFGB in the reference plane $z = 1000\lambda$. $N = 5$ and $w_0 = 0.5\lambda$: **a** $\langle S_z \rangle_{\mathrm{TE}}$, **b** $\langle S_z \rangle_{\mathrm{TM}}$, **c** $\langle S_z \rangle$

References

1. J. Serna, P.M. Mejfas, R. Martinez-Herrero, Proc. SPIE **1834**, 162 (1992)
2. S.A. Amarande, Opt. Commun. **129**, 311 (1996)
3. V. Bagini, R. Borghi, F. Gori, A.M. Pacileo, M. Santarsiero, D. Ambrosini, G.S. Spagnolo, J. Opt. Soc. Am. A **13**, 1385 (1996)
4. R. Borghi, M. Santarsiero, S. Vicalvi, Opt. Commun. **154**, 243 (1998)
5. Y. Cai, Q. Lin, J. Opt. A, Pure Appl. Opt. **5**, 272 (2003)
6. H. Mao, D. Zhao, F. Jing, H. Liu, X. Wei, J. Opt. A, Pure Appl. Opt. **6**, 640 (2004)
7. H. Jiang, D. Zhao, Z. Mei, Opt. Commun. **260**, 1 (2006)
8. L. Hu, Y. Cai, Phys. Lett. A **360**, 394 (2006)
9. X. Lu, Y. Cai, Opt. Commun. **269**, 39 (2007)
10. B. Lü, S. Luo, B. Zhang, Opt. Commun. **164**, 1 (1999)
11. M. Ibnchaikh, A. Belafhal, Opt. Commun. **193**, 73 (2001)
12. N. Zhou, G. Zeng, L. Hu, Opt. Commun. **240**, 299 (2004)
13. X. Ji, B. Lü, Optik **114**, 394 (2003)
14. M. Alavinejad, B. Ghafary, F.D. Kashani, Opt. Laser Eng. **46**, 1 (2008)
15. Y. Cai, J. Opt. A, Pure Appl. Opt. **8**, 537 (2006)
16. H.T. Eyyuboğlu, C. Arpali, Y. Baykal, Opt. Express **14**, 4196 (2006)
17. Y. Cai, J. Opt. A, Pure Appl. Opt. **10**, 075003 (2008)
18. Y. Baykal, H.T. Eyyuboğlu, Appl. Opt. **45**, 3793 (2006)
19. Y. Baykal, H.T. Eyyuboğlu, Appl. Opt. **46**, 5044 (2007)
20. D.W. Coutts, IEEE J. Quantum Electron. **38**, 1217 (2002)
21. F. Wang, Y. Cai, Opt. Lett. **33**, 1795 (2008)
22. M.S. Bowers, Opt. Lett. **17**, 1319 (1992)
23. M.R. Perrone, A. Piegari, IEEE J. Quantum Electron. **29**, 1423 (1993)
24. G. Duplain, P.G. Verly, J.A. Dobrowolski, A. Waldorf, S. Bussiére, Appl. Opt. **32**, 1145 (1993)
25. J. Ojeda-Castañeda, G. Saavedra, E. Lopez-Olazagasti, Opt. Commun. **102**, 21 (1993)
26. F. Gori, Opt. Commun. **107**, 335 (1994)
27. Y. Cai, Q. Lin, J. Opt. A, Pure Appl. Opt. **6**, 390 (2004)
28. Y. Li, Opt. Lett. **27**, 1007 (2002)
29. Y. Li, Opt. Commun. **206**, 225 (2002)
30. X. Chu, Y. Ni, G. Zhou, Opt. Commun. **274**, 274 (2007)
31. X. Chu, Z. Liu, Y. Wu, Appl. Phys. B **92**, 119 (2008)
32. M.A. Porras, Opt. Commun. **127**, 79 (1996)
33. R. Martínez-Herrero, P.M. Mejías, S. Bosch, A. Carnicer, J. Opt. Soc. Am. A **18**, 1678 (2001)
34. G. Zhou, Appl. Phys. B **93**, 891 (2008)
35. G. Zhou, Opt. Lett. **31**, 2616 (2006)
36. D. Deng, Q. Guo, Opt. Lett. **32**, 2711 (2007)
37. I.S. Gradshteyn, I.M. Ryzhik, *Table of Integrals, Series, and Products*, corrected and enlarged edn. (Academic Press, New York, 1980)
38. G.P.M. Poppe, C.M.J. Wijers, ACM Trans. Math. Softw. **16**, 38 (1990)
39. P.C. Chaument, J. Opt. Soc. Am. A **23**, 3197 (2007)
40. G. Zhou, Opt. Express **16**, 3504 (2008)
41. W.H. Carter, J. Opt. Soc. Am. **62**, 1195 (1972)
42. J.D. Joannopoulis, R.D. Meade, J.N. Winn, *Photonic Crystals* (Princeton University, Princeton, 1995)
43. A. Ciattoni, B. Crosignani, P.D. Porto, Opt. Commun. **202**, 17 (2002)